ANALYSIS OF DYNAMIC TENSILE DEFORMATION CHARACTERISTICS OF DEEP COAL ROCK

L.G. Miao [1,2], B.M. Shi[1], Y.Y. Niu[3]

[1]School of Mining and Safety Engineering, An Hui University of Science and Technology, Huainan, 232001, China.
[2]College of Energy and Transportation Engineering,
Jiangsu Vocational Institute of Architectural Technology, Xuzhou, 221116, China
[3]College of Rail Transit, Jiangsu Province Xuzhou Technician Institute,
Xuzhou, 221000, China.

ABSTRACT

In order to study the dynamic tensile deformation failure characteristics of deep coal rock, the impact loading system of Split Hopkinson Pressure Bar (SHPB) was used to carry out the Brazilian disc-splitting test under the impact for the deep coal rock samples. The influences of impact speed and bedding angle in the coal samples on the dynamic tensile strength, failure strain and strain rate of coal samples were discussed. The results showed that the larger the impact speed is, the larger the dynamic tensile strength is, but its increase gradually decreases with the impact speed increasing. The failure strain of coal samples is the maximal as the impact speed is 3.3 m/s. With the same impact speed, when, the bedding is vertical to the loading direction; the failure strain of coal rock is relatively larger. However, the strain rate is the smallest. Simultaneously, when the bedding is parallel or vertical to the loading direction, the tensile failure appears in the coal samples, but if the bedding is not parallel or vertical to the loading direction, there would appear the matrix tension and the shear failure of bedding together.

KEYWORDS: *Hopkinson Pressure Bar; Brazilian disc; splitting test; dynamic tension; stress wave*

1.0 INTRODUCTION

In recent years, with the decrease in shallow resources, the deep coal resources were gradually exploited, and so high-stress disturbance brought a severe challenge to the safe mining (Xie Heping, 2012). As one of the hotspots in rock mechanics study, the dynamic tensile strength of coal rock has important

---

* Corresponding Email: lgmiao1984@163.com

significance for the studies of stability control of coal rock, parameter selection of blasting works, the mechanism of percussive ground pressure, and so on (Miao Leigang, 2017). However, it is significantly difficult to directly stretch the coal rock. So the SHPB was used to conduct the dynamic splitting tensile test on the disc samples, which has been an easy and effective method to study the dynamic mechanical property of coal samples. Moreover, this method was used by scholars at home and abroad to test the static tensile mechanical properties for different types of rocks, and thus obtaining the tensile strength and failure characteristics of rocks, and so on (Zhao Na, 2015); Yang Zhipeng, 2015; You Mingqing, 2011; Li Guo, 2015).

Xu Jinyu (2014) has tested the dynamic tensile mechanical properties of plagioclase amphibolite, sericite-quartz schist, sandstone, and their results showed that the tensile mechanical property of rocks had a stronger strain rate sensitivity. Then, Song Xiaolin (2005) has found that the dynamic tensile strength increased with the increase of the strain rate through the dynamic Brazilian disc test. Likewise, the findings of Dai F (2010) and Dai F (2009) showed that the loading rate could effectively improve the dynamic tensile strength of granite through some tests. Man Ke (2010) has tested the dynamic fracture toughness and single axial tensile strength of basalt in different depths, as well as their relationship was quantitatively analyzed.

Furthermore, Li Diyuan (2015) tested the dynamic mechanical properties of yellowish sandstone, and showed that the influence results of bedding angle on the dynamic tensile strength. However, there were fewer studies on the tensile strength test of coal under dynamic loading. Moreover, there were primary structures such as bedding in the coal, which made discreteness of test results from SHPB increase. Hence, it is necessary to study the influence of bedding in the coal on the dynamic splitting tensile failure characteristics (Xia K W, 2010).

This paper analyzed the dynamic tensile characteristics of coal by dynamic Brazilian disc splitting test, carried out the impact splitting test by SHPB for disc-shaped coal samples, and discussed the dynamic response characteristics of impact speed and bedding angle of coal samples. Moreover, the deformation failure process of coal samples was observed by high-speed camera, as well as the deformation failure characteristics images of coal sample surface were recorded during the impact loading process.

2.0   EXPERIMENTAL

2.1   Samples preparation

The coal samples were from 13-1 coal layer in the Zhangji coal mine in Huainan, and the dynamic instability of coal rock often happened due to the larger mining pressure on the coal layer surface. In order to ensure a relevance between physical and mechanical characteristics of coal samples, all the coal samples were from a piece of complete coal. The size of coal sample for the test was Φ50mm × 25mm, the non-parallelism of two end faces after polish was no more than ± 0.02 mm. Moreover, the two end faces were vertical to the axis, and the maximal deviation was no more than 0.25°, as shown in Figure 1. Simultaneously, the uniaxial compressive strength of samples in 13-coal layer was 18 MPa, the elasticity modulus was 2.78 GPa, and the Poisson ratio was 0.226.

Fig.1. Preparation for coal samples

2.2   Test system

The Brazilian disc-splitting test of coal rock was completed in the SHPB system in the impact laboratory of Anhui University of Science and Technology, as shown in Figures 2 and 3. The diameter of steel cylindrical bullet of SHPB was 75 mm, and its length was 400 mm. The diameters of both steel input and output bars were 75 mm, their lengths were 4,000 mm and 2,500 mm, respectively. The material was high-strength alloy steel, and the elasticity modulus was 195GPa. The strain gauges were pasted on the places about 1m away from the sample ends of input and output bars, and the bar strain in the test process was recorded. The types of strain meter used in the experiment were BX120-2AA resistance strain gauge and HU101B-120 semiconductor strain gauge, and the electrical signals of strain gauge were processed and collected by DHHP-20 ultra-dynamic data acquisition system. The initial speed of bullets was controlled by gas pressure in the air chamber, and the input bar was measured

by photoelectric method.

Fig. 2. Test equipment of SHPB
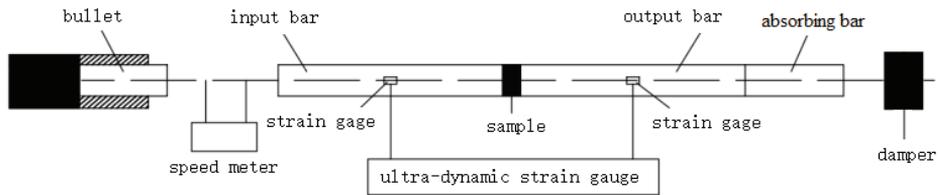
Fig.3. Diagram of test equipment system

2.3 Data processing

Based on the one-dimensional stress wave theory, the parameters of samples such as internal stress, strain and so on, were calculated by using the data of the incident wave and reflected wave on the left ends of samples as well as the transmitted wave on the right ends. The Brazilian disc sample linearly contacted with the bar, and the diameter of the sample was far less than the length of the impact bar. Moreover, when the strain rate was less than 10^3 s^{-1}, the dynamic constitutive relationship of rock materials was the same as the static constitutive relationship. Hence, the stress average of two ends of the sample can be regarded as the stress of the whole sample.

The strain $\varepsilon_s(t)$, strain rate $\dot{\varepsilon}_s(t)$, and stress $\sigma_s(t)$ of samples under the impact load are expressed in Equations (1) to (3) as follows:-

$$\varepsilon_s(t) = \frac{u_1(t) - u_2(t)}{D} = \frac{c_0}{D} \int_0^t [\varepsilon_I(t) - \varepsilon_R(t) - \varepsilon_T(t)] dt \tag{1}$$

$$\dot{\varepsilon}_s(t) = \frac{d\dot{\varepsilon}_s(t)}{dt} = \frac{c_0}{D} \int_0^t [\varepsilon_I(t) - \varepsilon_R(t) - \varepsilon_T(t)] dt \tag{2}$$

$$\sigma_s(t) = \frac{p_1(t) + p_2(t)}{2\pi DB} = \frac{EA}{2\pi DB} [\varepsilon_I(t) + \varepsilon_R(t) + \varepsilon_T(t)] \tag{3}$$

where E was the elasticity modulus and was 195 GPa. The term A was the cross-section area. D was the diameter of sample and was 75 mm. The term B was the sample thickness and was 30 mm. c_0 was the elastic wave velocity of bars and was 5000 m/s. Furthermore, $\varepsilon_I(t)$ was the incident strain signal of left end of the sample. $\varepsilon_R(t)$ was the reflected strain signal of left end of the sample. $\varepsilon_T(t)$ was the transmitted strain signal of right end of the sample.

In addition, the values of stress and strain were positive as the samples were compressed. Strain gauge signal of each bar in the SHPB output the voltage-time curve. In the test, the original waveform easily fluctuated due to the influence of test conditions, the low-pass filtering method was used to process data, and then each dynamic mechanical parameter of coal samples was figured out according to the results after processing. The typical incident, reflected and transmitted waveforms were shown in Figure 4. Simultaneously, the high-speed camera was used to shoot the destruction process of coal samples by impact load to obtain the distribution characteristics of surface strain field of coal samples during the dynamic splitting.
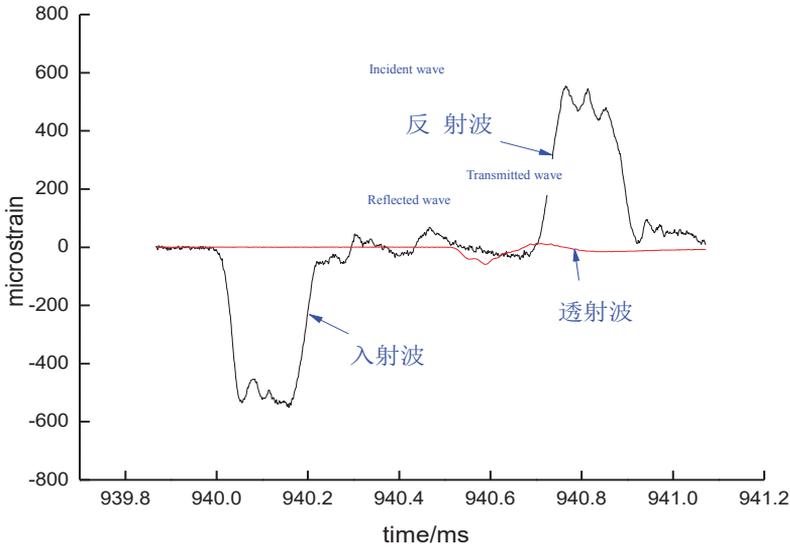
Figure 4. Typical stress waveform curve

3.0 RESULTS AND DISCUSSION

3.1 Response of dynamic tensile characteristics to impact speed

In the response characteristics of dynamic tensile strength to the impact speed, the change of dynamic tensile strength of coal samples with the impact speed was shown in Figure 5(a). It is found that when the impact speed was between 2.0 and 4.0 m/s, the dynamic tensile strength was between 4.30 and 5.90 MPa, which was 2.14 ～ 3.26 times larger than the static tensile strength.
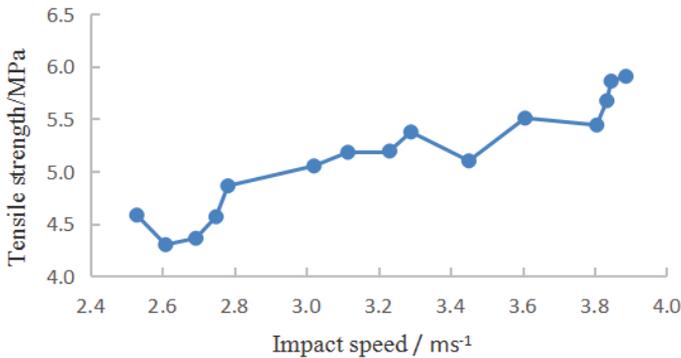
Figure 5(a). Dynamic tensile strength

In general, the dynamic tensile strength of coal samples increased with impact speed increasing, furthermore, as every 0.5 m/s increase in the impact speed, the dynamic tensile strength would increase by 10% ~ 20%. However, with the increase of impact speed, the increase range of dynamic tensile strength was more and more obvious. Figures 5(b) and (c) showed the changes of failure strain and strain rate with the impact speed, respectively. It can be clearly seen that the failure strain first increased then decreased with the impact speed, namely, the impact speed was between 2.0 and 4.0 m/s, the failure strain increased with the impact speed increasing. When the impact speed was more than 3.3 m/s, the failure strain would decrease with the increase of impact speed. The reason was that when the impact speed was more than 3.3 m/s, the larger impact force made the coal samples destroyed before deformation. Moreover, when the impact speed was between 2.0 and 4.0 m/s, the failure strain was between 550×10^{-6} and 750×10^{-6}, and the strain rate was between 45 and 80 s^{-1}. The strain rate rose with fluctuations with the increase of impact speed, namely, with the increase of impact speed, the strain rate first increased then decreased, subsequently decreased again.
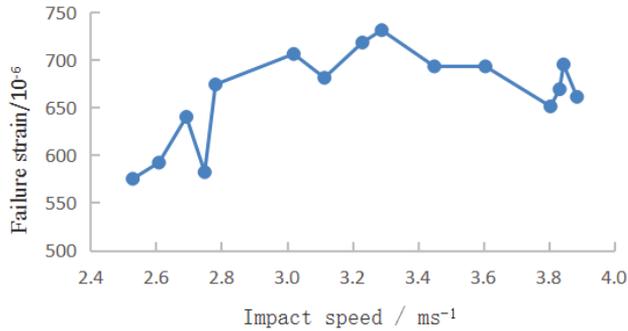
(b)
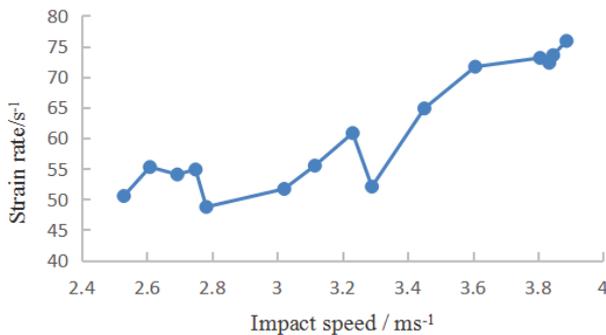
(c)

Figure 5(b) and (c). Change of dynamic tensile parameters (failure strain and strain rate) of coal samples with impact speed

3.2   Response characteristics of dynamic tensile properties to bedding of coal samples

With the same impact speed, there still existed difference in the dynamic mechanical properties of coal samples due to the influence of bedding in the coal samples. In consideration of the fluctuation of impact speed, the impact speeds close to each other were selected from the experimental results for grouping, and each coal sample contained five kinds of bedding angles as far as possible (namely, the angles θ between the bedding and loading direction was 0, 25.5°, 45.0°, 65.5° and 90.0°, respectively.), as shown in Figure 6. For the impact speed of three groups of coal samples and their bedding angles, the average impact speeds were 2.67 m/s, 3.22 m/s and 3.796 m/s, respectively.
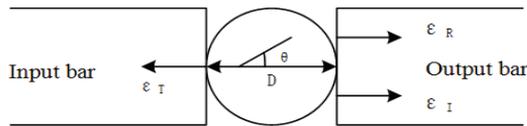
Figure 6. Diagram of sample loading by SHPB

Figure 7 showed the changes of dynamic tensile strength, failure strain and strain rate of coal samples with the bedding angle. Figure 7(a) showed that the larger the impact speed was, the larger the dynamic tensile strength of coal sample was. This suggested that the main influence factor of dynamic tensile strength was the impact speed rather than the bedding angle. When the impact speeds were the same as well as the bedding was vertical to the loading direction, the dynamic tensile strength was larger. Moreover, as the bedding angle was 25.5°, the dynamic tensile strength of three groups of coal samples was lower.

The change of the failure strain with the bedding angle shown in Figure 7(b). The failure strain of three groups of coal samples was between 540×10^{-6} and 720×10^{-6}. With the increased of bedding angle, the failure strain of coal samples generally increased, namely, with the bedding angle increasing, the coal samples failure transformed from tensile failure of bedding to the tensile-shear coupling failure of matrix and bedding. Furthermore, as the bedding was vertical to the loading direction, the coal sample failure was mainly the tensile failure of the matrix. The tensile failure of bedding was the easiest, and the

failure strain of coal samples was the smallest. The tensile failure for the matrix was the most difficult, and then the failure strain of coal samples was larger. At the average impact speed around 3.22 m/s, the failure strain of each bedding angle was higher than those under the other impact conditions. The results showed that the response of failure strain of coal samples to the impact was higher than that of failure strain to the bedding angle of coal samples.

Figure 7(c) showed the curve of relationship between the strain rate and bedding angle. When the impact speed was larger (the average speed was 3.796 m/s), the strain rate of coal samples was slightly affected by bedding angle. However, when the impact speed was smaller (the average speed was 3.2m/s and 2.6 m/s.), the strain rate changed with the fluctuation of bedding angle. Furthermore, when the bedding angle was 25.5°, the strain rate was the maximum among the strain rates responding to the other bedding angles with the same impact speed. This suggested that the coal sample was easily destroyed. At the bedding angle was 90°, the strain rate was lower, which showed that it was difficult to split the coal samples.

(a) Dynamic tensile strength of coal samples
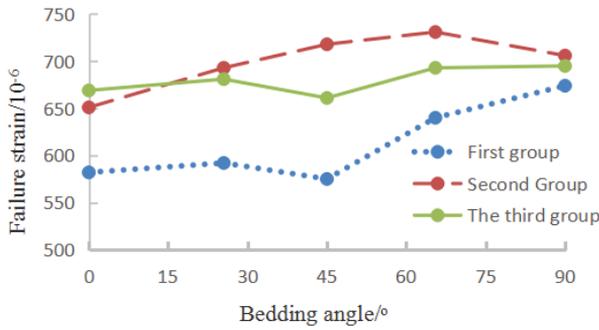
(b) Dynamic failure strain of coal samples
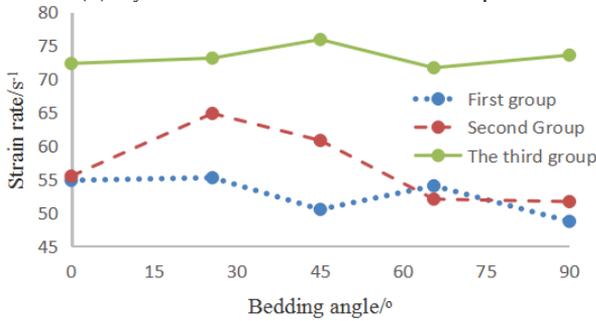
(c) Strain rate of coal samples

Figure 7. Relationship between dynamic tensile failure parameters and bedding angles of coal samples.

Figure 8 showed the pictures from high-speed camera of the dynamic failure progress of coal samples in the impact tests with different bedding angles. The bedding angles of coal samples obviously affected the splitting process under dynamic conditions. When the bedding was vertical and parallel to the incident direction, the coal sample failure was mainly the tensile split along the

loading direction. However, when there existed an angle between the bedding and incident direction (not vertical or parallel), the ways of coal failure were not only the tensile splitting along the incident direction but also the shear failure along the bedding direction.

| Contacting | 27μs | 55μs |
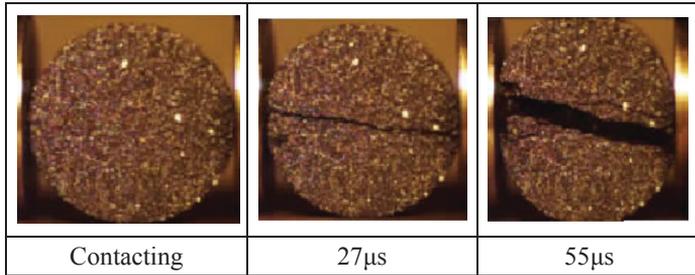
(a) The bedding angle was 0°.
(The coal sample *No.21* with an impact speed of 3.115 m/s).

| Contacting | 27μs | 55μs |
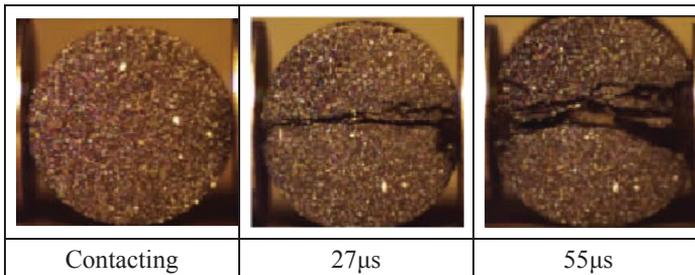
(b) The bedding angle was 45°
(The coal sample *No.23* with an impact speed of 3.231 m/s)

| Contacting | 27μs | 55μs |
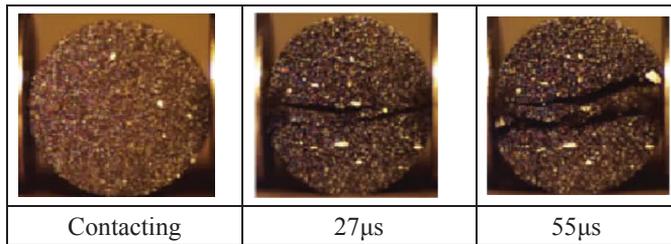
(c) The bedding angle was 90°
(The coal sample *No.25* with an impact speed of 3.021 m/s)

Figure 8. Impact splitting failure characteristics with different bedding angles.

This suggested that the tensile failure of matrix was accompanied by the shear failure of bedding. Moreover, the crack in coal samples mostly started along the incident direction under the impact load, and then many micro cracks

appeared around the locations where the samples contacted with the input and output bars. Subsequently, the micro cracks converged, intersected, and finally, the samples fractured.

With the gradual increase of sample deformation, the sample fractured slowly in the bedding, and thus forming the final fracture surface. It is worth noting that the extension path of cracks was not smooth due to the influence of bedding surface, and so the coal samples would strip and decompose along the bedding surface.

4.0   CONCLUSIONS

The dynamic tensile strength of coal samples increased with the increase of impact speed. As every 0.5 m/s increase in the impact speed between 2.0 and 4.0 m/s, the dynamic tensile strength would increase by 10% $\sim$ 20%. However, with the impact speed increasing, the increase of dynamic tensile strength obviously slowed. The failure strain reached the maximum as the impact speed was 3.3 m/s, but subsequently, the failure strain decreased with the increase of impact speed. The strain rate rose with the fluctuations with the impact speed.

The response of dynamic tensile characteristics to the impact speed was obviously higher than the response to the change of bedding angle in the coal samples. When the impact speeds were the same as well as the bedding was vertical to the impact direction, the dynamic tensile strength was larger. However, when the bedding angle was 25.5°, the dynamic tensile strength was smaller. With the bedding angle increasing, the failure strain generally increased. As the bedding angle increased, the coal samples failure transformed from tensile failure of bedding to the tensile-shear coupling failure of matrix and bedding. Furthermore, when the bedding was vertical to the loading direction, the coal sample failure was mainly the tensile failure of the matrix. When the impact speed was larger, the strain rate was slightly affected by the bedding angle.

The crack in coal samples mostly started along the incident direction under the impact load, and then many micro cracks appeared around the locations where the samples contacted with the input and output bars. Subsequently, the micro cracks converged, intersected, and finally, the samples fractured. The extension

path of cracks was not smooth due to the influence of bedding surface. Hence, the bedding can directly affect the dynamic deformation of samples, but with the increase of the loading speed, the influence of bedding would decrease.

ACKNOWLEDGMENTS

REFERENCES

Dai F, Xia K, 2010. Loading rate dependence of tensile strength anisotropy of barre granite. *Pure and Applied Geophysics,* 167 (11):1419-1432.

Dai F, Chen R, Xia K, (2009). A semi-circular bend technique for determining dynamic fracture toughness. *Experimental Mechanics,* 50(6):783-791.

Dai F, Xia K, Tang L, (2010). Rate dependence of the flexural tensile strength of Laurentian granite. *International Journal of Rock Mechanics and Mining Sciences*, 47(3):469 -475.

Li Diyuan, Qiu Jiadong, Li Xibing, (2015). Experimental study on dynamic tensile and compressive properties of bedding sandstone under impact loading. *Chinese Journal of Rock Mechanics and Engineering*, 34(10):2091 - 2097.

Li Guo, Ai Ting, Yu Bin, (2015).Acoustic emission characteristics of different lithologies under Brazilian splitting. *Journal of China Coal Society*, 40(4):870-881.

Man Ke, Zhou Hongwei, (2010). Research on dynamic fracture toughness and tensile strength of rock at different depths. *Chinese Journal of Rock Mechanics and Engineering*, 29(8):1657-1663.

Miao Leigang, Shi Biming, Qin Ruxiang, (2017). Reasonable position and drainage effect of high-level drainage roadway in 13-1 coal seam of Liuzhuang Coal Mine. *Coal Engineering,* 49(4):7-9.

Song Xiaolin, Xie Heping, Wang Qizhi, (2005). Failure strain of Brazilian disc samples of marble under dynamic split tests. *Chinese Journal of Rock Mechanics and Engineering*, 40(16):2953 -2959.

Xia K W, Huang S, Jha A K, (2010). Dynamic tensile test of coal, shale and sandstone using split Hopkinson pressure bar: A tool for blast and impact assessment. *International Journal of Geotechnical Earthquake Engineering*, 1(2):24-37.

Xie Heping, Zhou Hongwei, Xue Dongjie, Wang Hong-Wei,Zhang Ru,Gao Feng, (2012). Research and consideration on deep coal mining and critical mining depth. *Journal of China Coal Society*, 37 (4):535-542.

Xu Jinyu, Liu Shi, Sun Huixiang, (2014). Analysis of dynamic split tensile tests of flattened Brazilian disc of three rocks. *Chinese Journal of Rock Mechanics and Engineering*, 49 (S1):2814-2819.

Yang Zhipeng, He Bai, Xie Lingzhi (2015). Strength and failure modes of shale based on Brazilian test [J]. Rock and Soil Mechanics, 36(12) : 3447-3455.

You Mingqing, Chen Xianglei, Su Chengdong, (2011). Brazilian splitting strengths of discs and rings of rocks in dry and saturated conditions. *Chinese Journal of Rock Mechanics and Engineering*, 30 (3):464-472.

Zhao Na, Wang Laigui, Xi Yanhui, (2015). Experiment study of crack propagation and strain evolution of Brazilian disc mudstone specimen. *Journal of Experimental Mechanics*, 30(6):791-796.